Heliyon 10 (2024) e39985

Contents lists available at ScienceDirect

Heliyon

journal homepage: www.cell.com/heliyon

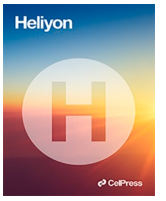

Research article

Effects of climate warming and declining water quality on the eco-environmental evolution of Jinmucuo Lake: Evidence from sedimentary diatom assemblages

Yu-rong Li [a,b], Yang Wang [a,b], Chun Ye [a,b], Zi-jian Xie [a,b,*], Chun-hua Li [a,b,**], Wei-wei Wei [a,b]

[a] National Engineering Laboratory for Lake Pollution Control and Ecological Restoration, Chinese Research Academy of Environmental Sciences, Beijing, 100012, China

[b] State Environmental Protection Key Laboratory for Lake Pollution Control, Chinese Research Academy of Environmental Sciences, Beijing, 100012, China

ARTICLE INFO

Keywords:
Diatom assemblage
Climate change
As pollution
Sediment core
Lake ecological degradation
Tibetan plateau

ABSTRACT

The problem of lake pollution on the Tibetan Plateau has become prominent in recent years because of the warming climate and increased human activity. However, it is difficult to obtain effective indicators to explain the long-term eco-environmental changes in plateau lakes. In this study, a sediment core from Jinmucuo Lake was taken as the research object, and the ^{210}Pb and ^{137}Cs isotopes, diatom assemblages, and climatic and environmental factors were analyzed. The results revealed that the lake had a sedimentation rate of 0.47 cm/a, and the age of the 30-cm sediment core was approximately 1876 AD. Diatom abundances at different ages tend to decrease. During 1876–1999, abundant diatom species, such as *Cymbella lanceolata*, *Navicula* sp., *Surirella ovalis*, *Synedra* sp., *Epithemia adnata*, *Cymbella pusilla*, *Amphora ovalis* and *Tabularia tabulata*, which included oligotrophic, mesotrophic, and eutrophic indicator species were detected, and the dominant species were *Cymbella lanceolata*, *Navicula* sp., *Surirella ovalis* and *Synedra* sp. After 2000, diatoms declined dramatically, and were undetected in most samples. Similarly, the species richness and Shannon–Wiener index plummeted to 0 in approximately 2002. Canonical correspondence analysis revealed that total nitrogen and organic matter were the main influencing factors of diatom assemblages before 2000, whereas As and mean annual temperature were the main influencing factors after 2000. These findings indicate that diatom habitats have been rapidly destroyed by increasing temperatures and As inputs, even in the presence of abundant nutrients in the lake.

1. Introduction

The Tibetan Plateau is the largest plateau in the world and has many lakes [1]. As an important part of the plateau ecosystem, lakes

* Corresponding author. Chinese Research Academy of Environmental Sciences, National Engineering Laboratory for Lake Pollution Control and Ecological Restoration, State Environmental Protection Key Laboratory for Lake Pollution Control, Beijing, 100012, China

** Corresponding author. Chinese Research Academy of Environmental Sciences, National Engineering Laboratory for Lake Pollution Control and Ecological Restoration, State Environmental Protection Key Laboratory for Lake Pollution Control, Beijing, 100012, China.

E-mail addresses: xiezijian@craes.org.cn (Z.-j. Xie), lich@craes.org.cn (C.-h. Li).

https://doi.org/10.1016/j.heliyon.2024.e39985
Received 17 June 2024; Received in revised form 17 October 2024; Accepted 23 October 2024
Available online 30 October 2024

on the Tibetan Plateau cover an area of 41831.7 km^2, accounting for 51.4 % of China's lake area [1]. Since the 1990s, China has focused primarily on addressing the water environmental pollution of freshwater lakes in densely populated and economically developed areas [2–4]. In recent years, the plateau region has experienced rapid development in secondary and tertiary industries, significantly improving the economy of the Tibetan Plateau [5]. Correspondingly, the economic development has also led to an increase in pollutant emissions [5,6]. Moreover, the Tibetan Plateau is located in a complex climatic and geothermal zone, and natural environmental changes significantly affect the lake ecosystems on the Tibetan Plateau, particularly for saltwater lakes that lack hydrodynamic cycles and are more vulnerable [7,8]. However, little research has been conducted on the evolution law of the ecological environment and its driving factors in inland saltwater lakes on the Tibetan Plateau.

Long-term systematic monitoring is crucial for understanding the evolutionary history of the lake ecological environment [9,10]. Nevertheless, most lakes lack such data. Paleolimnological methods employ multi-index analyses of sediment records to comprehensively reconstruct and quantitatively invert the history of long-term lake environmental changes and ecological responses [10]. For example, the diatom fossil proxies can be used to evaluate long-term response characteristics under different environmental stresses such as nutrients or temperature, making them a reliable indices for assessing changes in the lake ecosystems [9,11]. However, studies have focused mainly on freshwater lakes, leaving a gap in understanding the changing characteristics of plateau saltwater lakes.

Generally, nutrients are thought to be a major factor in the growth of diatoms [12,13]. An increase in nutrients is the main cause of eutrophication in most freshwater lakes, which affects the growth, reproduction and succession of diatoms, and then controls the eutrophication process in lakes [14]. On the Tibetan Plateau, lakes are not only affected by nutrient increases, but are also stressed by continuously elevated levels of arsenic (As) and fluoride (F). Studies have shown that As pollution can lead to strong changes in the composition of herbivores and diatoms, and diatoms contaminated with As for a long time are more tolerant to As [15,16]. Excessive F in water can accumulate in diatoms [17], which affects their metabolism of nucleotides and nucleic acids, and then affects the division process and photosynthesis of diatoms, thus posing a potential threat to the lake ecosystem [18,19]. Owing to the extreme climate conditions of the plateau and the unitary nutrient structure of the lakes, the plateau lake ecosystem is more sensitive to environmental changes than the traditional lake ecosystems [20,21]. Many scholars have focused on the impact of plateau climate change on diatoms in plateau lakes. For example, Song et al. [22] reported that the change in the diatom assemblage in Tingming Lake, Yunnan, was caused mainly by climate warming, and Liao et al. [23] reported that the response of diatoms to regional temperature changes was synchronous based on correlation analysis. However, the synergistic effects of the environment and climate change on diatom assemblage succession in plateau lakes have not been studied.

Jinmucuo Lake is a typical inland saltwater lake on the Tibetan Plateau. The ecological environment has been deteriorated due to socioeconomic development and extreme climatic effects, including the continuous increase in nutrients, As and F. In addition, the lake area has changed significantly over the past 50 years under the extreme climate of the Tibetan Plateau [24]. However, owing to the limited long-term water quality and biological monitoring data, coupled with the complex geographical and climatic environment, the research on the evolution of the lake ecological environment is laking. This study uses sediment cores from Jinmucuo Lake as the research object, and use paleolimnological methods, 1) to calculate the sediment deposition rates and ages; 2) to analyze shifts in diatom assemblages at different ages; 3) to explore the changes in climate and environmental factors at different ages; and 4) to determine the major factors affecting the evolution of diatom assemblages under conditions of constant increases in nutrients, As and F, and apparent changes in climate.

2. Materials and method

2.1. Study area

Jinmucuo Lake is located in Angren County, Shigatze City, on the southern Tibetan Plateau. The lake has an area of 22.4 km^2, and a basin area of 182.9 km^2. The elevation of the lake is 4301 m, and the mean depth is approximately 8.5 m, with a maximum depth of 15.3 m. The water capacity of the lake is 1.75×10^8 m^3. The tributaries in the watershed are mainly seasonal. Precipitation and snowmelt are the main sources of water for the lake. Grassland is the leading land use type in the basin, covering an area of 150 km^2.

The area has a semiarid climate in the plateau temperate zone. The mean annual temperature in the basin varies from 4.2 °C to 6.4 °C. Since the 1980s, temperatures in the region have shown an extremely significant increasing trend at a rate of 0.52 °C/10a (Fig. 2a), which is 2.9–3.7 times higher than the global warming rate (0.14 °C/10a~0.18 °C/10a) and 1.4 times higher than the mean warming rate of the Tibetan Plateau (0.36 °C/10a) [25,26]. The mean annual wind speed is 2.42 m/s, with variations ranging from 1.61 to 3.15 m/s (Fig. 2a). The mean annual precipitation and evaporation are 294 mm and 2513 mm, respectively (Fig. 2b). Rainfall occurs mostly from June to September. The mean annual snow depth is 4.78 cm (Fig. 2c). The GDP of Angren County has had an increasing trend, increasing from 98 million CNY in 2000 to 1.3 billion CNY in 2021 (Fig. 2d). The villages in the in Jinmucuo Lake Basin include Jiangga village, Zhelong village, Kaga village, and Snow village. The total population of the watershed is 2516, of which 219 people are urban and 2297 people are rural.

According to the topography and water system composition of the Jinmucuo Basin, combined with regional land use and administrative division characteristics, the grid distribution of the entire lake was determined. A total of 20 lake water sample collection points were arranged in Jinmucuo Lake, and water sample collectors were used to collect water samples 0.5 m below the surface. pH and salinity were measured with a multiparameter water quality analyzer (YSI 6600V2, USA). The transparency of each sample was measured via a Secchi disc. The total nitrogen (TN) content was determined via the alkaline potassium persulfate digestion UV spectrophotometric method [27]. The total phosphorus (TP) content was determined via the ammonium molybdate spectrophotometric method [28]. The chemical oxygen demand was determined via the dichromate method [29]. F was determined by F

reagent spectrophotometry [30]. As was determined by atomic fluorescence spectrometry [31]. According to the results of a water quality survey in 2023, the physical and chemical characteristics of the water in Jinmucuo Lake are shown in Table 1. The pH is strongly alkaline, with a high salinity. Most notably, the lake has high concentrations of not only nutrients, including TP and TN but also As and F.

2.2. Sample collection and laboratory analysis

Lake sediment cores are crucial for extracting information about lake sediment disturbances. In September 2023, two sediment cores were taken from the Jinmucuo Lake via UWITEC sampling equipment, one of which had a uniform texture, and clear layers were used for further analysis (Fig. 1). Moreover, water samples from 20 sampling sites for water sample were collected and analyzed (Fig. 1; Table 1).

The sediment was divided at intervals of 1 cm after collection, then sealed with polyethylene bags and promptly brought back to the laboratory for refrigeration at −4 °C for subsequent analysis and testing. The laboratory analysis items included radioactive element (^{210}Pb, ^{226}Ra, and ^{137}Cs) activity; TN, TP, mass susceptibility, and diatoms; and 21 other types of geochemical elements (K, Ca, Na, Mg, Fe, Ti, Sr, Mn, As, Ba, Be, Cu, Pb, Li, Ni, Sb, Mo, V, Cr, Zn, and Ti).

The activities of ^{210}Pb, ^{226}Ra and ^{137}Cs were determined via gamma spectrometry with well-type coaxial low background intrinsic germanium detectors (GWL-120-15, USA). K, Ca, Na, Mg, Fe, Ti, and TP were determined via ICP-OES (Agilent 5110, USA). Sr, Mn, As, Ba, Be, Cu, Pb, Li, Ni, Sb, Mo, V, Cr, Zn, and Ti were determined via ICP-MS (NexlON 1000G, UK). As was determined by AFS (AFS-933, CHN). The organic matter content was determined via the external heating method with potassium dichromate oxidation. The TN content was determined via the semimicro Kelvin method. The diatom fossil samples in the sediments were processed via standard methods [32–34]. In detail, approximately 0.5 g of dry sediment was heated in a water bath at 80 °C with 10 % HCl and 30 % H_2O_2 added successively to dissolve carbonate and digest organic matter, respectively. After each sample was washed with distilled water in a centrifuge three times, it was dried on cover slips and mounted onto permanent glass microscope slides with Naphrax mounting medium. Species identification was based on the classification system of Krammer and Lange-Bertalot [14,35,36]. Counting and identification of diatoms were carried out under the oil mirror of a Zeiss Axio Scope A1 optical microscope (magnification 100 × 10). The number of valves in sediment surface samples was not less than 500, and the number of valves in the other samples was not be less than 300.

2.3. Data analysis

2.3.1. Chronological sequence reconstruction method

^{137}Cs is an artificial radionuclide, and large-scale nuclear tests worldwide were conducted in 1963; therefore, the peak concentration of ^{137}Cs in the sediment core depth profile typically corresponds to the maximum deposition from atmospheric sources in 1963 [37]. In this study, the core chronology was determined via the composite model of constant rate of supply (CRS) dating model. The results of the CRS calculations were corrected by using a model with a ^{137}Cs timescale to obtain the true borehole age scale [38].

(1) The calculation formulas for the ^{137}Cs timescale and the corresponding ages after 1963 is as follows:

$$T_m = T_0 + \lambda^{-1} n1 + (A_0 - A_m) P^{-1} \lambda]$$

$$P = \frac{-\lambda (A_0 - A_w)}{1 - e^{-\lambda (T_0 - 1963)}}$$

$$A_w = \sum_{x=w}^{n} C_x \rho_x$$

(2) The formula for calculating the corresponding ages of the following levels before 1963 is as follows:

Table 1
Physical and chemical characteristics of the water in Jinmucuo Lake.

Item	Unit	Mean value	Variation range
pH	–	9.88	9.86–9.94
salinity	ppt	4.19	3.90–4.22
Transparency	cm	22	15~30
Total phosphorus	mg L^{-1}	3.29	2.49–3.85
Total nitrogen	mg L^{-1}	2.30	1.41–2.87
Chemical oxygen demand	mg L^{-1}	116	64~157
Floride	mg L^{-1}	8.9	7.1–10.5
Arsenic	mg L^{-1}	0.097	0.056–0.150

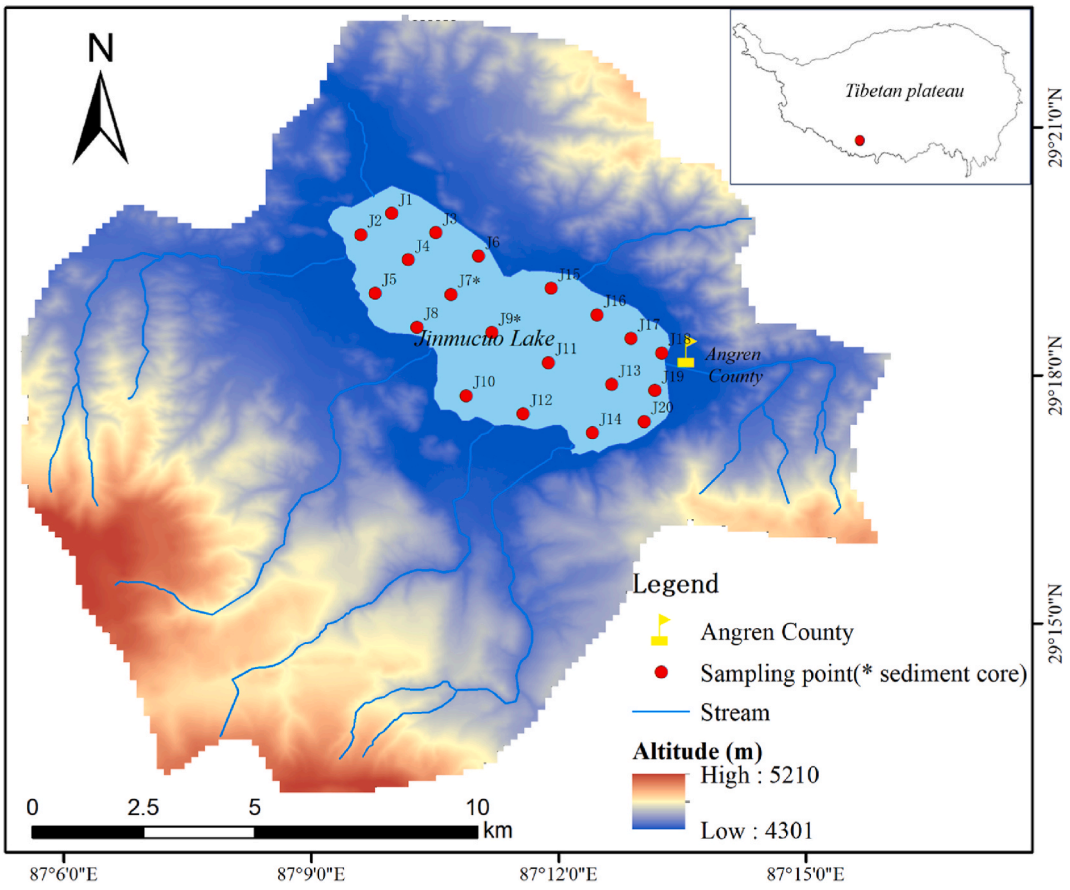

Fig. 1. Geographical location of the study area and the layout of the sampling points.

$$T_m = 1963 - \lambda^{-1} \ln\left(A_w A_m^{-1}\right)$$

where T_m is the age corresponding to a depth of m. T_0 is the sampling year. λ is the decay constant of ^{210}Pb (0.03114). A_0 is the $^{210}Pb_{ex}$ cumulant of the entire sediment core (Bq/cm^2). A_m is the $^{210}Pb_{ex}$ cumulant below a depth of m (Bq/cm^2). A_w is the $^{210}Pb_{ex}$ cumulant below the w horizon corresponding to 1963 (Bq/cm^2). C_x is the $^{210}Pb_{ex}$ activity at x depth (Bq/kg), and x is the sample bulk weight at x mass depth (g/cm^2).

2.3.2. Diatom abundance calculation

The absolute abundance of a diatom is usually its total quantity, which is calculated via the following formula [39]:

$$B = \frac{\left(N \times \frac{A}{a}\right) \times \frac{V}{v}}{W}$$

B represents the absolute abundance of a diatom (valves/g), N represents the number of diatoms observed, A is the total area of the slide, a is the area observed, V represents the volume of the diatom liquid after extraction, v represents the volume of the liquid containing diatoms dropped on the cover slide, and W represents the dry weight of the sediment.

The analysis data of diatom assemblages are usually expressed in terms of the relative abundance of each species, which is calculated as follows [39]:

$$F_i = \frac{N_i}{N} \times 100\%$$

F_i represents the relative abundance of i species, N_i is the number of i species, N is the total quantity of the diatom of sample.

2.3.3. Analysis of dynamic changes in diatom assemblages and extraction of driving factors

Species that appeared in at least two samples and contained more than 5 % of the samples were selected for square root conversion. The environmental factors were first transformed by $\log_{10}(x+1)$, and then the following analysis was performed. The dynamic changes

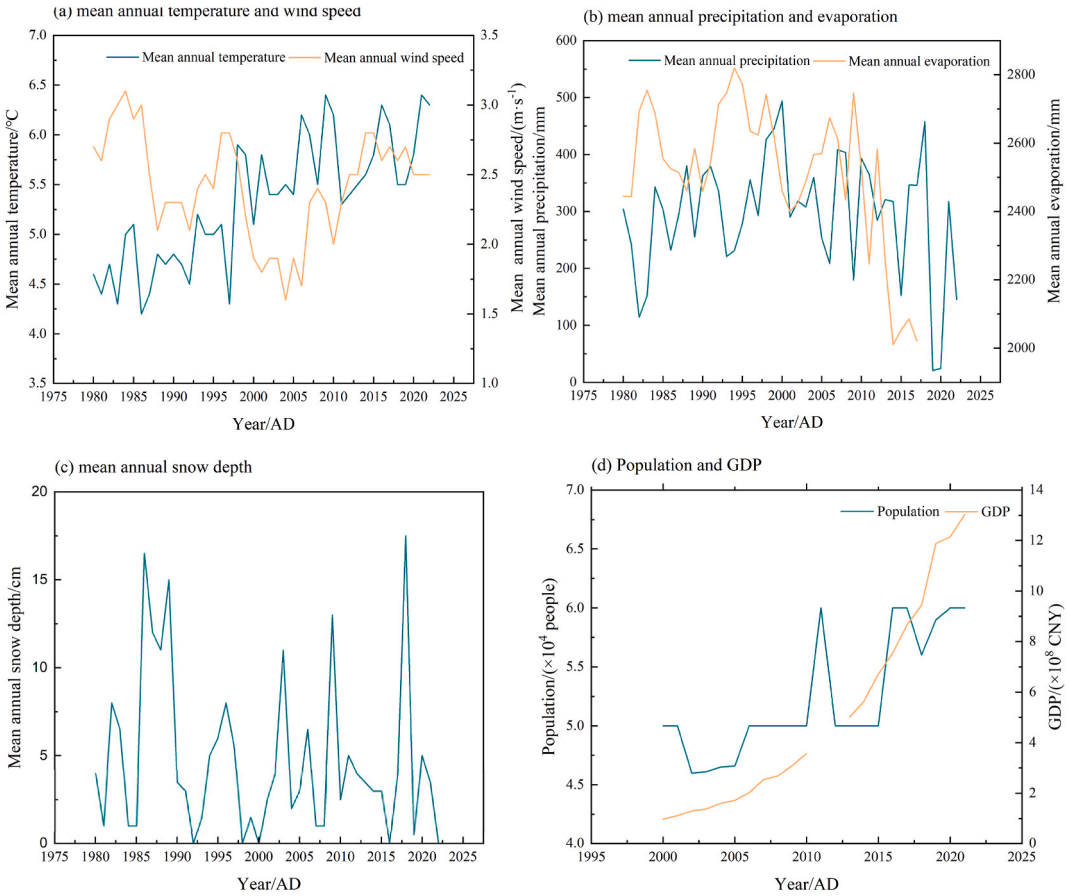

Fig. 2. Trends of climatic and socioeconomic data in Angren County: (a) mean annual temperature and wind speed; (b) mean annual precipitation and evaporation; (c) mean annual snow depth.

in the diatom assemblages were extracted by detrending correspondence analysis (DCA). If the gradient length of the DCA is greater than 4 standard deviation (SD) units, the unimodal methods are more suitable. If it is less than 3, the linear model is more appropriate. If it is between 3 and 4, both models can be used. DCA revealed that the length of the first axis was 7.21 (>4) standard units, and canonical correspondence analysis (CCA) was selected for analysis.

In the process of CCA, environmental factors with high collinearity (VIF>10) were eliminated on the basis of the variance inflation factor (VIF), and environmental factors with high contribution rates were screened via forward selection. All analyses and all ordinations were performed via CANOCO 5.0 [40].

2.3.4. Species diversity analysis

The diversity of species is a crucial aspect of ecosystem complexity, and analyzing species-level diversity provides the most comprehensive insight into biodiversity, encompassing factors such as species threat status and endemism. There are also scholars who have applied it to the research of diatoms, concentrating on the altered trend of diatoms in response to human activities and climate change [41,42]. In this study, the diatom biodiversity of a sediment core was computed, emphasizing the variation characteristics of the diatom diversity of centennial species under anthropogenic and climatic alterations.

The diatom diversity was analyzed via the Shannon–Wiener Index [(H′)] and Species richness (S) as follows:

$$H' = -\sum_{i=1}^{S} P_i \log_2 P_i$$

$$P_i = \frac{n_i}{N}$$

$$S = n$$

where S represents the number of species in the sample. n_i is the individual number of the i species of the sample, N is the total number of individuals of the sample, and n is the total number of species types in the sample with a nonzero number of individuals.

2.3.5. Pearson correlation analysis

Species richness, the Shannon–Wiener index, the DCA Axis I score, the sediment indices (TN, TP, As, F, Pb, Cu, Fe/Mn, organic matter, and magnetic susceptibility), the mean annual temperature, the mean annual precipitation, the mean annual evaporation, the mean annual wind speed and mean annual snow depth in the Jinmucuo Basin were determined via Pearson correlation analysis. The major factors affecting the diatom assemblage diversity and the environmental factors significantly correlated with the first axis score of the DCA were identified.

3. Results

3.1. Establishment of the chronological sequence of the sediment

As shown in Fig. 3a, the average specific activity of ^{137}Cs in the Jinmucuo sediment core was 8.41 Bq/kg, with variability ranging from 0 to 14.09 Bq/kg. The specific activity of ^{137}Cs was a single accumulation peak, and the accumulation peak occurred at a depth of 19 cm (14.09 Bq/kg), corresponding to the nuclear test peak in 1963. The average specific activity of $^{210}Pb_{ex}$ is 60.10 Bq/kg, ranging from 20.01 to 112.70 Bq/kg (Fig. 3a). The specific activity of $^{210}Pb_{ex}$ in the Jinmucuo sediment core had an irregular sawtooth distribution and an exponential decline, indicating that the sedimentation rate in the study area varied with time.

According to the CRS model, the age of the sediment core at 30 cm was approximately 1876 AD, and the average deposition rate and sediment flux were 0.47 cm/a and 0.34 g/cm^2/a, respectively (Fig. 3b). Specifically, the average sediment flux from 1876 to 1929 was 0.17 g/cm^2/a, with a variation range of 0.15–0.20 g/cm^2/a, and the average sediment flux from 1942 to 1970 was 0.25 g/cm^2/a, ranging from 0.20 to 0.28 g/cm^2/a. The average sediment flux from 1975 to 2004 was 0.33 g/cm^2/a, with an average range of 0.30–0.37 g/cm^2/a, and the average sediment flux from 2008 to 2022 was 0.59 g/cm^2/a, ranging from 0.43 to 0.91 g/cm^2/a. Overall, the sediment flux had an increasing trend with time, with little sediment flux before 2008, but a rapid increase from 2008 onward.

3.2. Characteristics of the diatom assemblages

As shown in Fig. 4, a total of 70 species of diatoms of 24 genera, mainly benthic and epiphytic types, were identified in the Jinmucuo sediment core. The main dominant taxa included *Achnanthes*, *Amphora*, *Cymbella*, *Diatomaceae*, *Epithemia*, *Fragilaria*, *Gomphonema*, *Navicula*, *Nitzschia*, *Rhopalodia*, *Surirella*, and *Synedra*. According to the distribution of diatoms in the sediment core, the species that appeared in two or more samples and had a relative abundance ≥5 % were selected as the main species of the diatom assemblages in Jinmucuo in the past 150 years. There were 23 species of diatoms, and the sum of the relative abundances of these diatoms in each sample ranged from 59.1 % to 100.0 %, with an average value of 83.2 %. Depending on the significant changes in the relative and absolute abundance of diatoms, it can be divided into two assemblage zones. The assemblage characteristics of diatoms are described below.

Zone I (11–30 cm, 1876–1999): During this period, the absolute abundance had a increasing trend from 1876–1942 (mean of 43,404 valves/g), and a fluctuating decreasing trend from 1942 to 1999 (mean of 37,145 valves/g). The dominant species were *Cymbella lanceolata*, *Navicula* sp., *Surirella ovalis* and *Synedra* sp., with relative abundances ranging from 0 to 16.07 %, 0–21.43 %, 0–43.72 % and 0–18.18 %, respectively. The mean relative abundances were 7.45 %, 7.74 %, 5.27 % and 6.43 %, respectively. Among them, *Cymbella lanceolata* is a typical eutrophic indicator species, and *Surirella ovalis* is a halophilic species. The relative abundance of the other three dominant species decreased with decreasing depth, except for *Synedra* sp. which increased with decreasing depth. There were also oligotrophic, mesotrophic indicator species were detected, such as *Epithemia adnata*, *Cymbella pusilla*, *Amphora ovalis*,

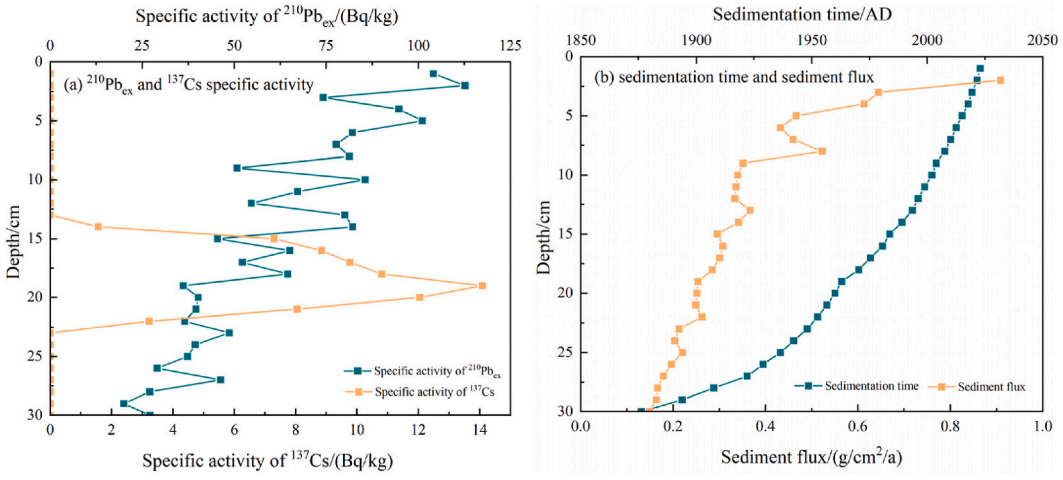

Fig. 3. Establishment of the chronological sequence of the sediment: (a) $^{210}Pb_{ex}$ and ^{137}Cs specific activity; (b) sedimentation time and sediment flux.

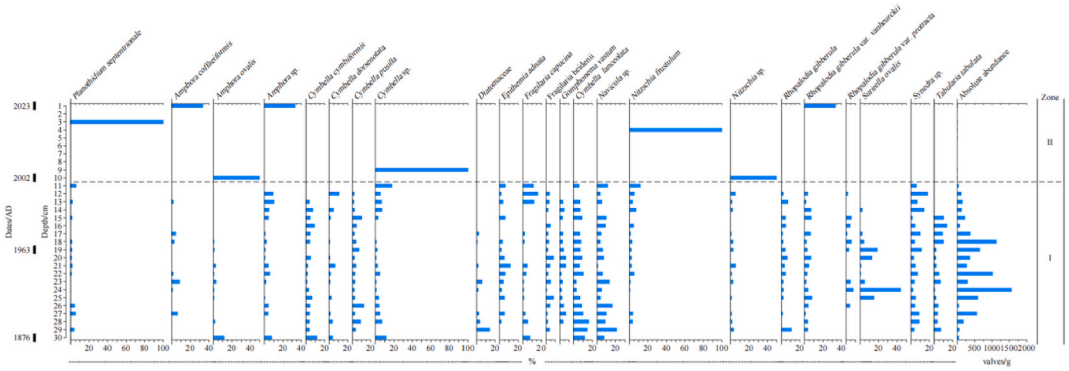

Fig. 4. Diagram of the assemblage variations in the dominant diatoms in the lake sediment core.

Rhopalodia gibberula, *Rhopalodia gibberula* var. *vanheurckii* and *Rhopalodia gibberula* var. *protracta*, the mean relative abundances were 3.08 %, 3.93 %, 1.11 %, 2.83 %, 3.67 % and 1.94 %, respectively. The oligotrophic indicator species *Epithemia adnata* increased first and then decreased with decreasing depth, while the relative abundance of mesotrophic indicator such as species *Cymbella pusilla* and *Amphora ovalis* decreased, *Rhopalodia gibberula* var. *vanheurckii* and *Rhopalodia gibberula* var. *Protracta* increased. In addition, the relative abundance of the eutrophic indicator species *Fragilaria capucina* and eutrophic lake dominant species *Tabularia tabulata* increased with decreasing depth, ranging from 0 to 16.36 % and 0–13.64 %, respectively, with a mean abundance of 3.58 % and 4.08 %, respectively.

Zone II(1–10 cm, 2002–2023): During this period, the species type and number of lake diatoms decreased dramatically, with absolute abundances of only 0–806 valves/g and an mean abundance of 268 valves/g. Only nine species were detected during this period: *Planothidium septentrionale*, *Amphora coffaeiformis* var. *borealis*, *Amphora ovalis*, *Amphora* sp., *Cymbella* sp., *Nitzschia frustulum*, *Nitzschia* sp., *Rhopalodia gibberula* var. *vanheurckii*, and *Tetracyclus* sp. The dominant species in Zones I, such as *Cymbella lanceolata*, *Navicula* sp., *Surirella ovalis* and *Synedra* sp., all disappeared. Oligotrophic and mesotrophic indicator species, such as *Epithemia adnata*, *Cymbella pusilla* and *Amphora ovalis* also disappeared. Moreover, it is worth noting that most of the samples had no detectable diatoms or only had a single diatom species.

The DCA of the diatom assemblage data revealed that 21.23 %, 14.85 %, 5.44 % and 3.44 % of the diatom assemblage data were explained by the first four sorting axes, respectively. The first axis captures most of the information on diatom assemblage changes, indicating that diatom associations changed significantly in approximately 2002 (Fig. 4; Fig. 5). Succession in the diatom assemblages and the first axis score of the DCA indicated that the ecological environment in the Jinmucuo Lake has deteriorated since the beginning of the 21st century, with a sharp decrease in the diversity and abundance of algal species.

3.3. Diversity characteristics of diatom species

Overall, the species diversity of the diatom assemblages in the Jinmucuo Lake increased from 1876–1970, then decreased from 1970–1999, and finally declined dramatically after 2000 (Fig. 5). First, the diversity index had an increasing trend from 1876–1970 (corresponding to depths of 18–30 cm). Species richness ranged from 14 to 44, with an average value of 28.5, and the Shannon−Wiener

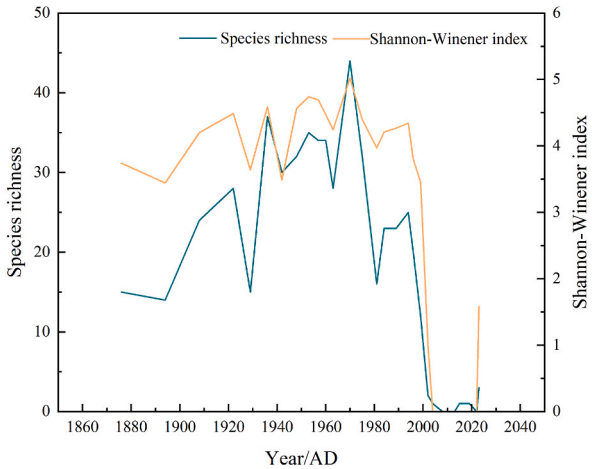

Fig. 5. Variation characteristics of diatom species richness and the Shannon−Weiner index.

index was ranged from 3.44 to 5.02, with a mean value of 4.25. The diversity index then had a downward trend from 1970 to 1999 (corresponding depths of 11–17 cm). Species richness ranged from 12 to 32 (mean 21.6), and the Shannon–Wiener index ranged from 3.45 to 4.40 (mean 4.06). The species richness and Shannon–Wiener index subsequently plummeted to 0 in approximately 2002, indicating that the habitat of diatoms in the Jinmucuo Lake has changed dramatically since the 21st century. From 2002–2023 (corresponding depths of 1–10 cm), the species richness ranged from 0 to 3, with a mean value of 0.9, and the Shannon–Wiener index ranged from 0 to 1.58, with a mean value of 0.26.

3.4. Characteristics of sedimentary geochemical indices

The sediment geochemical indicators truly recorded the long-term changes in Jinmucuo Lake. The TP concentration had a decreasing trend from 1876–1963 (mean of 664 ppm), and a fluctuating increasing trend from 1963 to 2023 (mean of 698 ppm); then, the growth rate increased significantly in 1996 and reached 700 ppm after 2000 (Fig. 6).

The TN and organic matter contents showed a similar trends. They were stable from 1876 to 1922, with an average values of 1.31×10^3 ppm and 18.88×10^3 ppm, respectively. Subsequently, rapid increases began in 1922, and peaked in 1942, at 2.95×10^3 ppm and 49.40×10^3 ppm, respectively. A decreasing trend was observed from 1942–2023, with mean values of 1.89×10^3 ppm and 27.57×10^3 ppm, respectively. In addition, As and F also showed similar trends. There was a slow downward trend from 1876 to 1960, and a fluctuating upward trend after 1960. As was lower than 40 ppm before 1975 and higher than 50 ppm after 1981, and then increased to 100 ppm in 2004. F was lower than 700 ppm before 1999, then increased to 700 ppm after 2002, and reached 804 ppm in 2023.

The Fe/Mn ratio is often used to reconstruct paleoclimate conditions in sedimentary areas [43,44]. Mn generally exists in water as Mn^{2+}. When environmental evaporation increases, the saturation concentration of Mn^{2+} decreases, and Mn^{2+} precipitates, resulting in Mn enrichment in the sediment. However, Fe is easily precipitates in colloidal form in water, and the Fe/Mn ratio is relatively high in warm and humid climates, whereas the ratio of Fe/Mn is relatively low in dry climates. The Fe/Mn values in Jinmucuo ranged from 30.5 to 41.8, with an average value of 36.6, indicating that the climate in the Jinmucuo Basin is arid and that the results are consistent with the reality that the Jinmucuo Basin is arid. However, the increasing trend of the Fe/Mn ratio in Jinmucuo Lake (Fig. 6) does not align with the decreasing trend of the annual rainfall in the basin (Fig. 2b), which might be attributed to alterations in the redox conditions of the sediment cores. Under oxidative conditions, Fe^{3+} and Mn^{4+} are insoluble, and Fe^{3+} and Mn^{4+} can be reduced to soluble Fe^{2+} and Mn^{2+} by bacteria under reducing conditions [45,46]. The calculation of the redox potential indicates that the reduction of Mn^{4+} precedes that of Fe^{3+} [47]; therefore, bacterial Mn reduction occurs in the shallower layer of the sediments. Consequently, as the sedimentary core gradually becomes anoxic, the Fe/Mn ratio in the sediment will gradually increases.

Magnetic susceptibility in sediments is often used to analyze the changes in the production pattern and intensity of human activity during the historical period of a basin, and to indicate the stability of the soil [48,49]. As shown in Fig. 6, the magnetic susceptibility gradually decreased to a stable trend from 1876 to 1960, ranging from 18.72×10^{-8} to 27.18×10^{-8} m^3/kg (mean of 21.34×10^{-8} m^3/kg). The magnetic susceptibility increased gradually from 1960–2002, with a range of 18.46–26.89×10^{-8} m^3/kg (mean of 22.06×10^{-8} m^3/kg). The magnetic susceptibility then tended to fluctuate, and the overall trend increased, with a range of $12.81 \times$

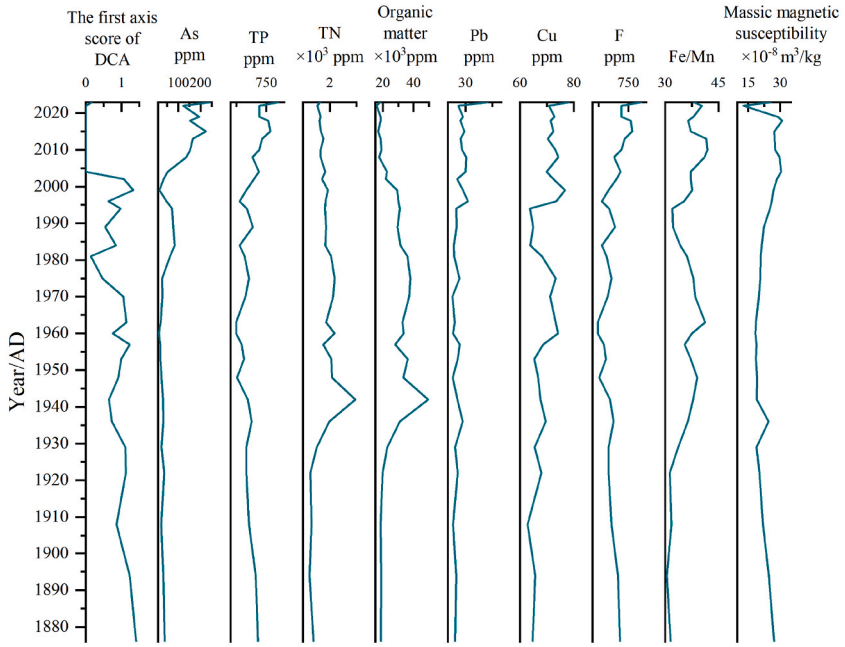

Fig. 6. Variation characteristics of multiple indices in the lake sediment core.

10^{-8}~30.96 × 10^{-8} m^3/kg (mean of 26.94 × 10^{-8} m^3/kg). Since the beginning of the 21st century, human activity has led to an increase in magnetic minerals entering the lake, and as a result, the magnetic susceptibility of Jinmucuo Lake has gradually increased over time.

3.5. Analysis of the driving factors of diatom assemblage changes

The CCA was performed on the basis of a combination of sediment physicochemical indices, climate data, and diatom data, and then, environmental factors with high contribution rates were selected via forward selection. The results revealed that TN, As, mean annual temperature, mean annual snow depth and organic matter were the five most significant factors affecting the succession of diatom assemblages over the last 40 years, contributing 25.9 %, 14.5 %, 15.9 %, 16.7 % and 27.1 %, respectively (Fig. 7).

The first two axes explained almost 44.9 % of the environment–species relationship. The first axis was positively correlated with the mean annual temperature and mean annual snow depth, and negatively correlated with As, TN, and organic matter. The second axis was positively correlated with the mean annual temperature and As, and negatively correlated with the TN, organic matter, and mean annual snow depth. The variables associated with the variability of the diatom assemblages explained by the environmental factors were organic matter (17.6 %), TN (16.9 %), mean annual snow depth (10.9 %), mean annual temperature (10.3 %) and As (9.4 %). According to the CCA sequencing diagram, TN and organic matter were the most important factors affecting the sample points before 2000. However, the most important factors affecting the sample points after 2000 were As and the mean annual temperature.

A correlation analysis of species richness, the Shannon–Wiener index, and the DCA Axis I score with sediment indicators and watershed climate data is shown in Fig. 8. Organic matter and mean annual evaporation were positively correlated with species richness and the Shannon–Wiener index, whereas As, F, TP and mean annual temperature were negatively correlated with species richness and the Shannon–Wiener index. Specifically, the correlations between organic matter and species richness, TP and the Shannon–Wiener index was highest, with correlation coefficients of 0.78 and −0.77, respectively. Additionally, the correlation coefficients between TP and species richness, As and the Shannon–Wiener index were −0.75 and −0.76, respectively. Moreover, the correlation coefficients of F with species richness and the Shannon–Wiener index were −0.74 and −0.75, respectively. The first axis score of the DCA was only significantly correlated with only As, with a correlation coefficient of −0.80.

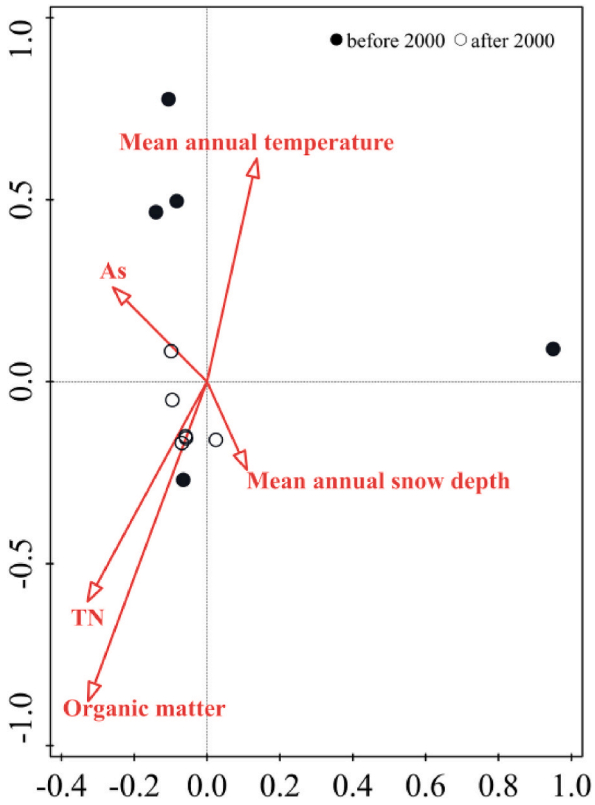

Fig. 7. Rank diagram of the CCA between sediment samples and environmental factors.

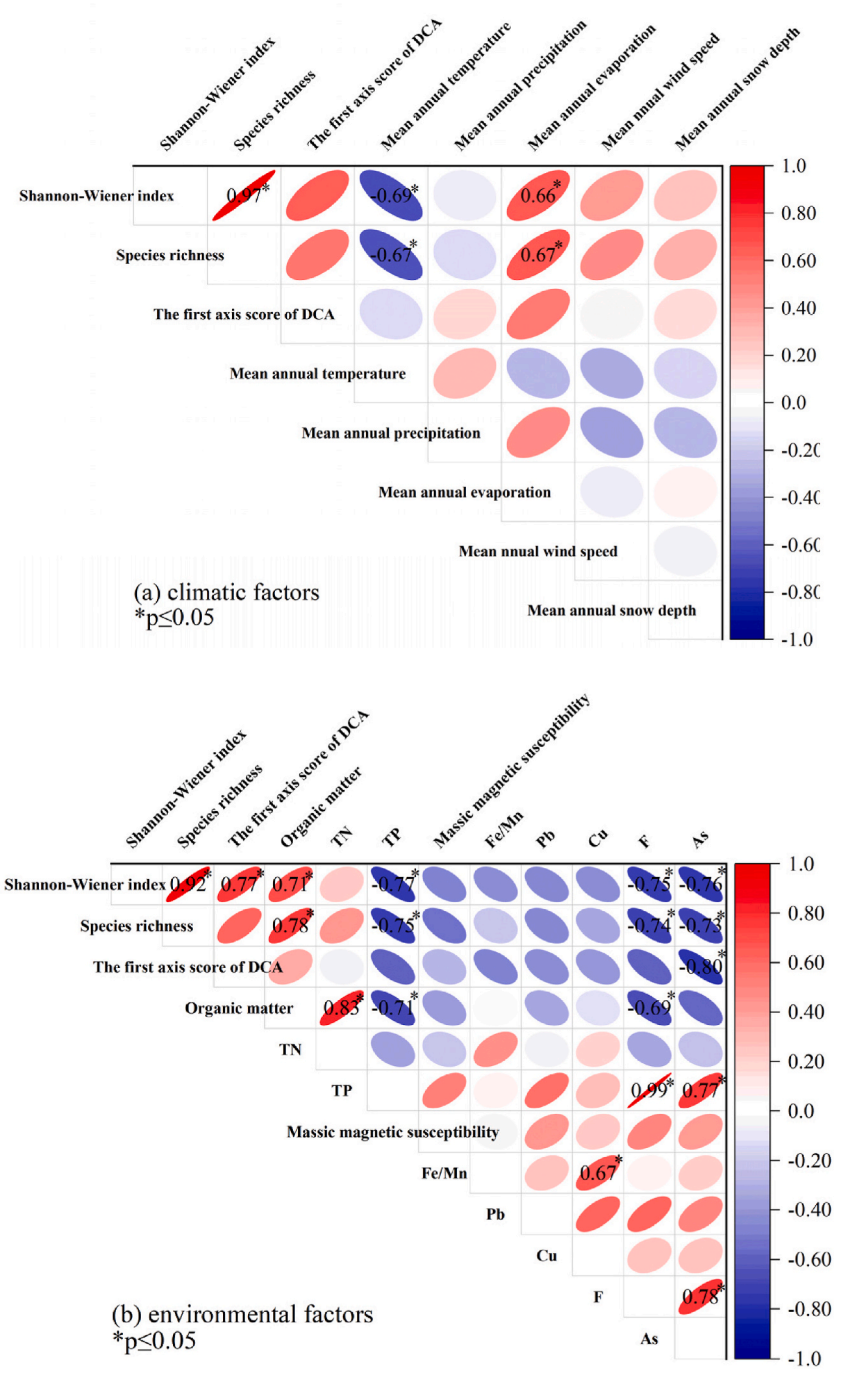

Fig. 8. The results of correlation analysis: (a) climatic factors; (b) environmental factors.

4. Discussion

4.1. *Effects of lake environmental changes on diatom assemblages*

Environmental conditions are the main influence on the succession in diatom assemblages. The time series of diatom assemblage changes reflects the long-term driving process of lake environment changes. Sedimentary diatom fossil records indicate that the dominant species in the Jinmucuo Lake diatom assemblages between 1876 and 1999 were *Cymbella lanceolata*, *Navicula* sp., *Surirella ovalis* and *Synedra* sp. The composition of diatoms can indicate lake eutrophication. Most mesotrophic lakes are dominated by *Navicula*,

which is consistent with the characteristics of the dominant species of Jinmucuo diatom during this period [50]. Moreover, *Cymbella lanceolata* is a typical eutrophic indicator species, suggesting that Jinmucuo Lake was in a eutrophic state at this time. Furthermore, *Fragilaria capucina* and *Tabularia tabulata* were also present during this period. *Fragilaria capucina* is an indicator species of eutrophication and *Tabularia tabulata* is also the dominant species in some eutrophic waters. Notably, the abundance of oligotrophic and mesotrophic species, such as *Epithemia adnata*, *Cymbella pusilla*, and *Amphora ovalis*, decreased during this time. In conclusion, over the past hundred years, the diatom assemblages in Jinmucuo Lake have shifted from oligotrophic species to eutrophic species. The dominant eutrophic species in Jinmucuo Lake are *Navicula, Rhopalodia* and *Synedra*, which differ from the dominant species in the middle and lower reaches of the Yangtze River, such as *Cyclotella meneghiniana*, *Cyclotella atomus*, *Stephanodiscus parvus*, *Stephanodiscus minutulus* and *Navicula subminiscula* [51]. This may be related to the fact that Jinmucuo Lake is a saltwater lake in a high cold region on the plateau, where the environment is selective for diatom growth and distribution. Moreover, the integrity of all sedimentary diatom assemblages is influenced to a certain extent by burial processes. In particular, diatoms deposited in saline lakes are frequently particularly susceptible to chemical and physical processes that result in poor preservation [52]. Flower and Ryves [53] investigated the preservation of diatom fossils from two salt lakes in the United States and Egypt and demonstrated that poor preservation of diatom fossils was often correlated with lower diatom content and higher salinity, and that sedimentation rate also influenced the preservation of diatoms.

On the one hand, CCA revealed that TN and organic matter explained 16.9 % and 17.6 %, respectively, of the long-term changes in the diatom assemblage structure. Additionally, organic matter and TP were strongly correlated with species richness and the Shannon–Wiener index. These findings indicate that nutrient levels drive long-term changes in diatom assemblage structure and diatom species diversity.

On the other hand, the diatom assemblages and species diversity shifted significantly during the periods of increased As and F contents in the sediment. The results of the Pearson correlation analysis revealed that As and F were the most important factors affecting the sample points. As was significantly negatively correlated with species richness, the Shannon–Wiener index and the DCA Axis I score ($p \leq 0.05$), whereas F was significantly negatively correlated with species richness and Shannon–Wiener index ($p \leq 0.05$). Similarly, both the species richness and the Shannon–Wiener index both started to decline significantly after 1981 and plummeted or disappeared well into the 21st century, which was essentially the same time point as the rapid increase in the As and F contents. Moreover, the mutation point of the DCA Axis I score was essentially the same as the time point at which the As content increased rapidly. Studies have shown that amorphous iron oxides featuring an unsaturated tetrahedral structure possess strong adsorption and capture capabilities for As [54]. The abrupt increase in As content in the core during the 2000s might have been associated with the adsorption of As by amorphous iron oxides at the sediment–water interface, suggesting severe As pollution in Jinmucuo Lake. As and F have significant effects on the growth and reproduction of diatoms. As pollution can lead to a large loss of herbivores and strong changes in the composition of algae. Algae that have experienced long-term As pollution have a greater tolerance to As, which can severely affect the health and stability of the ecosystem [15,16]. Excessive concentrations of F in water can accumulate in aquatic organisms, affecting the metabolism of nucleotides and nucleic acids, which in turn affects the division of algal cells and the photosynthesis in algae, thus posing a potential threat to the ecosystem [18,19]. Chen et al. [16] and Tao et al. [55] reported that high concentrations of As pollution might exert a certain inhibitory effect on certain diatoms, and that the shift in diatom assemblage is closely linked to the trajectory of As input, exhibiting characteristics similar to thoes of the evolution of Jinmucuo diatom assemblages. The addition of 50–200 mg/L F to nutritionally adequate sterile seawater inhibits the growth of *Chaetoceros gracilis*, but hardly affects the growth of *Thalassiosira weissflogii* [56,57]. Joy and Balakrishnan [58] reported that the growth of *Nitzschia palea* was promoted at a F concentrations ranging from 10–110 mg/L, whereas *Halamphora coffeiformis* was significantly stimulated at F concentrations higher than 70 mg/L, and its growth declined rapidly. The simultaneous increase in As and F in Jinmucuo Lake allowed diatoms to be subjected to tremendous pressure at the same time, resulting in a dramatic decrease in diatom diversity when the concentrations of As and F reached a certain level.

Generally, nutrients are considered to be the main factor affecting the growth of diatoms. For Jinmucuo Lake, the TP concentration in the sediment core was relatively high after the 1960s (Fig. 6). From 1876–1963, the TP content in the sediment core continued to decline, with a mean of 664 ppm. From 1960–2023, the TP content continuously increased, with a mean of 698 ppm. The CCA results revealed that TN and organic matter were the main influences before 2000, but these effects began to weaken after 2000. The main reason may be that the nutrients were always in a sufficient state during this period; therefore, nutrients were not the limiting environmental factors of diatoms. On the other hand, As was the main influencing factor affecting samples after 2000, and the DCA Axis I score was only significantly correlated with only As according to the Pearson correlation analysis ($p \leq 0.05$). Although nutrients play an important role in influencing diatom assemblages, their role is replaced by the deleterious effects of As when the concentration increases to a certain level.

4.2. Effect of climate change on diatom assemblages

Climate change is a key factor affecting the growth of diatom assemblages. Owing to the extreme environmental conditions and the unitary nutrient structure of lakes on the plateau, lake ecosystems on the plateau are more sensitive to environmental changes than the traditional lake ecosystems [20,21]. The CCA results revealed that the mean annual snow depth and mean annual temperature were the most significant factors affecting the variability of the diatom assemblage data, accounting for 10.9 % and 10.3 % of the diatom assemblage variability, respectively. Moreover, Pearson correlation analysis revealed that species richness and the Shannon–Wiener index were significantly negatively correlated with mean annual temperature, and significantly positively correlated with annual evaporation, respectively ($p \leq 0.05$, Fig. 8).

Under the effects of global warming, the mean annual snow melt and precipitation in the Jinmucuo Basin increased, whereas the mean annual evaporation decreased. The Fe/Mn ratio is often used to reconstruct paleoclimate conditions in sedimentary areas [43,44]. The Fe/Mn ratios indicated that the climate in the Jinmucuo Basin is arid. Climate warming will enhances the thermal stratification of water bodies, thus weakening the vertical mixing of water bodies [59]. A decrease in surface wind speed can intensify the thermal stratification of water bodies, resulting in the weakening of water mixing, indirectly affecting the light and nutrient conditions in water bodies, and causing changes in aquatic assemblages [59,60]. Saline lakes in closed basins represent the end point for exogenous organic matter and nutrients. A steady stream of shore-sourced materials, including microorganisms, organic matter and minerals, is imported into the Jinmucuo Lake through precipitation, snowmelt, and runoff, resulting in a relative reduction in water transparency and an increase in nitrogen and phosphorus nutrient loads.

Moreover, the increase in precipitation and decrease in evaporation has caused changes in the water level and area of Jinmucuo Lake. Over the past 50 years, the area of Jinmucuo Lake has obviously changed [24]. In the first stage, the lake area decreased significantly from 23.62 km^2 to 18.18 km^2 from the 1970s–1995. The lake area expanded to 21.85 km^2 between 1995 and 2010. The lake area subsequently decreased again to 20.51 km^2 during the 2010–2015 period. After 2015, the lake area has increased and stabilized at 22.4 km^2. The lake area in Jinmucuo has experienced shrinkage, expansion and stabilization over the past 50 years, which has also affected lake water dynamics and water exchange, and has had some impact on the habitat of diatoms. As a result, the dominant species in Jinmucuo are predominantly those that are tolerant of turbid and nutrient-rich water, as well as mixed and stirred shallow water, such as *Synedra* sp., *Tabularia tabulata*, *Cymbella lanceolata*, *Navicula* sp., and *Surirella ovalis* [61,62]. This indicates that under the effect of global warming, reduced evaporation under the premise of increased snowmelt and precipitation indirectly leads to frequent water disturbances and turbidity over a long period, which further affects the changes in the diatom assemblages in the Jinmucuo Lake.

5. Conclusion

This study focused on the effects of the lake environment and climate indicators on the evolution of diatom assemblages and water eutrophication in Jinmucuo Lake, a typical saltwater lake on the Tibetan Plateau. The results of the CRS model revealed that the multiyear sedimentation rate of the lake was 0.47 cm/a and that the age of the 30 cm sediment core was approximately 1876 AD. The abundance of diatoms during different historical periods had a downward trend. During 1876–1999, abundant diatom species, such as *Cymbella lanceolata*, *Navicula* sp., *Surirella ovalis*, *Synedra* sp., *Epithemia adnata*, *Cymbella pusilla*, *Amphora ovalis* and *Tabularia tabulata*, which included oligotrophic, mesotrophic, and eutrophic indicator species were detected, and the dominant species were *Cymbella lanceolata*, *Navicula* sp., *Surirella ovalis* and *Synedra* sp. After 2000, the number of diatoms has declined dramatically, and diatoms or single diatom species were not detected in most samples. Similarly, the species richness and Shannon–Wiener index plummeted to 0 in approximately 2002. The CCA results revealed that TN and organic matter were the main influencing factors for samples before 2000, whereas As and mean annual temperature were the main influencing factors for samples after 2000. These results indicated that diatom habitats are rapidly destroyed by increasing temperatures and the input of As, even in the presence of abundant nutrients in the lake.

In the future, more biological indicators, such as branch horn and midge shells, should be included for a comprehensive analysis, because different organisms may respond differently to specific environmental stresses. Furthermore, more studies on the impact of continuous As input on the ecological environment of plateau lakes are recommended, which is crucial for improving the ecological quality of plateau lakes.

CRediT authorship contribution statement

Yu-rong Li: Writing – original draft, Methodology, Investigation, Formal analysis, Conceptualization. **Yang Wang:** Investigation, Formal analysis. **Chun Ye:** Supervision, Methodology, Conceptualization. **Zi-jian Xie:** Writing – review & editing, Validation, Supervision, Investigation. **Chun-hua Li:** Writing – review & editing, Supervision, Resources. **Wei-wei Wei:** Resources, Investigation.

Data availability

Data will be made available on request.

Declaration of competing interest

The authors declare the following financial interests/personal relationships which may be considered as potential competing interests:Zijian Xie reports financial support was provided by National Natural Science Foundation of China (No. 42307037), the National Key Research and Development Project (No. 2021YFC3201502), and the Jinmucuo Lake pollution source tracing project. Zijian Xie reports a relationship with Chinese Research Academy of Environmental Sciences that includes: employment. If there are other authors, they declare that they have no known competing financial interests or personal relationships that could have appeared to influence the work reported in this paper.

Acknowledgments

This research was funded by the National Natural Science Foundation of China (No. 42307037), the National Key Research and Development Project (No. 2021YFC3201502), and the Jinmucuo Lake pollution source tracing project.

References

[1] R. Ma, G. Yang, H. Duan, J. Jiang, S. Wang, X. Feng, A. Li, F. Kong, B. Xue, J. Wu, S. Li, China's lakes at present: number, area and spatial distribution, Sci. China Earth Sci. 54 (2) (2011) 283–289, https://doi.org/10.1007/s11430-010-4052-6.
[2] B. Qin, G. Gao, G. Zhu, Y. Zhang, Y. Song, X. Tang, H. Xu, J. Deng, Lake eutrophication and its ecosystem response, Chin. Sci. Bull. 58 (9) (2013) 961–970, https://doi.org/10.1007/s11434-012-5560-x.
[3] T. Fang, K. Yang, W. Lu, K. Cui, J. Li, Y. Liang, G. Hou, X. Zhao, H. Li, An overview of heavy metal pollution in Chaohu Lake, China: enrichment, distribution, speciation, and associated risk under natural and anthropogenic changes, Environ. Sci. Pollut. Control Ser. 26 (2019) 29585–29596, https://doi.org/10.1007/s11356-019-06210-x.
[4] X. Yan, Y. Xia, C. Ti, J. Shan, Y. Wu, X. Yan, Thirty years of experience in water pollution control in Taihu Lake: a review. Science of the Total Environment, Sci. Total Environ. 914 (2024) 169821, https://doi.org/10.1016/j.scitotenv.2023.169821.
[5] M. Wang, L. Yang, J. Li, Q. Liang, The evaluation and sources of heavy metal anomalies in the surface soil of eastern Tibet, Minerals 13 (1) (2023) 86, https://doi.org/10.3390/min13010086.
[6] N. Cai, X. Wang, H. Zhu, Y. Hu, X. Zhang, L.Q. Wang, Isotopic insights and integrated analysis for heavy metal levels, ecological risks, and source apportionment in river sediments of the Qinghai-Tibet Plateau, Environ. Res. 251 (2024) 118626, https://doi.org/10.1016/j.envres.2024.118626.
[7] C. Yu, Y. Sun, X. Zhong, Z. Yu, X. Li, P. Yi, H. Jin, D. Luo, Arsenic in permafrost-affected rivers and lakes of Tibetan Plateau, China, Environ. Pollut. Bioavailab. 31 (1) (2019) 226–232, https://doi.org/10.1080/26395940.2019.1624198.
[8] S. Shi, Q. Feng, H. Zhang, W. Zhao, J. Zhou, G. Zhu, Z. Niu, S. Zhang, Arsenic in Tibetan Plateau's geothermal systems: a detailed analysis of forms, sources, and geochemical behaviors, Discover Appl. Sci. 6 (4) (2024), https://doi.org/10.1007/s42452-024-05798-1.
[9] C. Dalton, J.P. Smol, Pollution of lakes and rivers: a paleoenvironmental perspective, 2nd edition, J. Paleolimnol. 42 (2009) 301–302, https://doi.org/10.1007/s10933-009-9320-0.
[10] E.D. Reavie, A.J. Heathcote, V.L.S. Chraïbi, Laurentian Great Lakes phytoplankton and their water quality characteristics, including a diatom-based model for paleoreconstruction of phosphorus, PLoS One 9 (8) (2014), https://doi.org/10.1371/journal.pone.0104705.
[11] L. Li, C. Li, C. Ye, Y. Chu, X. Li, Y. Zhang, H. Xian, Z. Xie, W. Wei, X. Dong, Nutrient history in the past century and its baseline of Xingkai Lake, J. Earth Environ. 13 (5) (2022) 557–570, https://doi.org/10.7515/JEE222028 (IN CHINESE).
[12] S. Liu, M. Yao, S. Chen, X. Yuan, Surface sediment diatom assemblages response to water environment in Dongping Lake, North China, Water 13 (3) (2021) 339, https://doi.org/10.3390/w13030339.
[13] L.L. Yuan, R.M. Mitchell, A. Pollard, C.T. Nietch, E.M. Pilgrim, N.J. Smucker, Understanding the effects of phosphorus on diatom richness in rivers and streams using taxon–environment relationships, Freshw. Biol. 86 (3) (2023) 473–486, https://doi.org/10.1111/fwb.14040.
[14] S. Blanco, C. Cejudo-Figueiras, L. Tudesque, E. Bécares, L. Hoffmann, L. Ector, Are diatom diversity indices reliable monitoring metrics? Hydrobiologia 695 (2012) 199–206, https://doi.org/10.1007/s10750-012-1113-1.
[15] K. Knauer, R. Behra, H. Hemond, Toxicity of inorganic and methylated arsenic to algal communities from lakes along an arsenic contamination gradient, Aquat. Toxicol. 46 (3–4) (1999) 221–230, https://doi.org/10.1016/S0166-445X(98)00131-3.
[16] G. Chen, H. Shi, J. Tao, L. Chen, Y. Liu, G. Lei, X. Liu, J.P. Smol, Industrial arsenic contamination causes catastrophic changes in freshwater ecosystems, Sci. Rep. 5 (2015) 17419, https://doi.org/10.1038/srep17419.
[17] S. Wang, J. Wang, X. Zhang, X. Xu, Y. Wen, J. He, Y. Zhao, Freshwater quality criteria of four strobilurin fungicides: interspecies correlation and toxic mechanism, Chemosphere 284 (2021) 131340, https://doi.org/10.1016/j.chemosphere.2021.131340.
[18] Canadian Council of Ministers of the Environment, Canadian water quality guidelines for the protection of aquatic life, Inorganic Fluorides (2001) 41. https://publications.gc.ca/collections/Collection/En1-34-3-2001E.pdf.
[19] Y. Chae, D. Kim, Y.J. An, Effect of fluoride on the cell viability, cell organelle potential, and photosynthetic capacity of freshwater and soil algae, Environ. Pollut. 219 (2016) 359–367, https://doi.org/10.1016/j.envpol.2016.10.063.
[20] J. Ren, X. Wang, C. Wang, P. Gong, X. Wang, T. Yao, Biomagnification of persistent organic pollutants along a high-altitude aquatic food chain in the Tibetan Plateau: processes and mechanisms, Environ. Pollut. 220 (2017) 636–643, https://doi.org/10.1016/j.envpol.2016.10.019.
[21] Y. Zhu, G. Chen, L. Kong, J. Li, X. Chen, P. Li, Q. Ma, Q. Zhou, L. Huang, Y. Ren, Long-term patterns of algal changes in response to climate change and atmospheric deposition in alpine lakes along the southeastern margin of Tibetan Plateau, J. Lake Sci. 35 (6) (2023) 2155–2169, https://doi.org/10.18307/2023.0651 (IN CHINESE).
[22] B. Song, L. Kong, Z. Hu, Q. Wang, X. Yang, Pollen and diatom record of climate and environmental change over the last 170 years in Tingming Lake, Yunnan Province, SW China, Quat. Int. 536 (2020) 85–91, https://doi.org/10.1016/j.quaint.2019.12.006.
[23] M. Liao, U. Herzschuh, Y. Wang, X. Liu, J. Ni, K. Li, Lake diatom response to climate change and sedimentary events on the southeastern Tibetan Plateau during the last millennium, Quat. Sci. Rev. 241 (2020) 106409, https://doi.org/10.1016/j.quascirev.2020.106409.
[24] G. Zhang, The Lakes Larger than 1 km2 in Tibetan Plateau (v3.1) (1970s-2022), National Tibetan Plateau/Third Pole Environment Data Center, 2019, https://doi.org/10.1016/j.scib.2019.07.018.
[25] G. Foster, S. Rahmstorf, Global temperature evolution 1979-2010, Environ. Res. Lett. 6 (4) (2011) 044022, https://doi.org/10.1088/1748-9326/6/4/044022.
[26] Y. Meng, K. Duan, P. Shi, W. Shang, S. Li, Y. Cheng, Li Xing, R. Chen, J. He, Sensitive temperature changes on the Tibetan Plateau in response to global warming, Atmos. Res. 294 (2023) 106948, https://doi.org/10.1016/j.atmosres.2023.106948.
[27] Chinese standard, Water Quality-Determination of Total Nitrogen-Alkaline Potassium Persulfate Digestion UV Spectrophotometric Method, HJ 636—2012, 2012 (IN CHINESE).
[28] Chinese standard, Water Quality-Determination of Total Phosphorus-Ammonium Molybdate Spectrophotometric Method, 1990. GB 11893-89. (IN CHINESE).
[29] Chinese standard, Water Quality-Determination of the Chemical Oxygen Demand-Dichromate Method, HJ 828—2017, 2017 (IN CHINESE).
[30] Chinese standard, Water Quality—Determination of Fluoride—Fluorine Reagents Spectrophotometry, HJ 488—2009, 2009 (IN CHINESE).
[31] Chinese standard, Water quality-determination of mercury, arsenic, selenium, Bismuth Antimony -Atomic Fluoresc. Spectr. HJ 694—2014 (2014) (IN CHINESE).
[32] R.W. Battarbee, V.J. Jones, R.J. Flower, N.G. Cameron, H. Bennion, L. Carvalho, S. Juggins, Diatoms, in: J.P. Smol, H.J.B. Birks, W.M. Last, R.S. Bradley, K. Alverson (Eds.), Tracking Environmental Change Using Lake Sediments, Developments in Paleoenvironmental Research, vol. 3, Springer, Dordrecht, 2002, https://doi.org/10.1007/0-306-47668-1_8.
[33] D.W. Morley, M.J. Leng, A.W. Mackay, H.J. Sloane, P. Rioual, R.W. Battarbee, Cleaning of lake sediment samples for diatom oxygen isotope analysis, J. Paleolimnol. 31 (3) (2004) 391–401, https://doi.org/10.1023/B:JOPL.0000021854.70714.6b.
[34] W. Zheng, E. Zhang, G.L. Peter, R. Wang, Systematic loss in biotic heterogeneity but not biodiversity across multiple trophic levels in Erhai lake, China, Sci. Total Environ. 906 (2024) 167479, https://doi.org/10.1016/j.scitotenv.2023.167479.
[35] K. Krammer, H. Lange-Bertalot, in: H. Ettl, J. Gerloff, H. Heynig, D. Mollenhauer (Eds.), Bacillariophyceae 1. Teil: Naviculaceae, 876 pp.; 2. Teil: Bacillariaceae, Epithemiaceae, Surirellaceae, 596 pp.; 3. Teil: Centrales, Fragilariaceae, Eunotiaceae, 576 pp.; 4. Teil: Achnanthaceae. Kritische Ergänzungen zu Navicula (Lineolatae) und Gomphonema, Süßwasserflora von Mitteleuropa Band 2/1-4, G. Fischer Verlag, Stuttgart, 1986–1991, p. 437.

[36] F. Córdoba, A.T. Luís, M. Leiva, A.M. Sarmiento, M. Santisteban, J.C. Fortes, J.M. Davila, O. Alvarez-Bajo, J.A. Grande, Biogeochemical indicators (waters/diatoms) of acid mine drainage pollution in the Odiel river (Iberian Pyritic Belt, SW Spain), Environ. Sci. Pollut. Res. 29 (21) (2022) 31749–31760, https://doi.org/10.1007/s11356-021-18475-2.
[37] A. Foucher, P.A. Chaboche, P. Sabatier, O. Evrard, A worldwide meta-analysis (1977-2020) of sediment core dating using fallout radionuclides including 137Cs and 210Pbxs, Earth Syst. Sci. Data 13 (10) (2021) 4951–4966, https://doi.org/10.5194/essd-13-4951-2021.
[38] E. Liu, B. Xue, X. Yang, Y. Wu, W. Xia, 137Cs and 210Pb chronology for modern lake sediment: a case study of Chaohu Lake and Taibai Lake, Mar. Geol. Quat. Geol. 29 (6) (2009) 89–94, https://doi.org/10.3724/SP.J.1140.2009.06089 (IN CHINESE).
[39] S. Liu, B. Li, L. Ran, R. Xu, K. Pang, Spring and autum (2020-2022) diatom composition of the surface sediments from the intertidal zone of Haimen, Nangtong, Acta Micropalaeontol. Sin. 41 (2) (2024) 174–184, https://doi.org/10.16087/j.cnki.1000-0674.20240510.001 (IN CHINESE).
[40] J. Lai, Canoco 5: a new version of an ecological multivariate data ordination program, Biodivers. Sci. 21 (6) (2013) 765–768, https://doi.org/10.3724/SP.J.1003.2013.04133 (IN CHINESE).
[41] R.M.M. Esposito, S.L. Horn, D.M. McKnight, M.J. Cox, M.C. Grant, S.A. Spaulding, P.T. Doran, K.D. Cozzetto, Antarctic climate cooling and response of diatoms in glacial meltwater streams, Geophys. Res. Lett. 33 (7) (2006), https://doi.org/10.1029/2006GL025903.
[42] S. An, D. Choi, J. Noh, High-throughput sequencing analysis reveals dynamic seasonal succession of diatom assemblages in a temperate tidal flat, Estuar. Coast Shelf Sci. 237 (2020) 106686, https://doi.org/10.1016/j.ecss.2020.106686.
[43] N. Tribovillard, T.J. Algeo, T. Lyons, A. Riboulleau, Trace metals as paleoredox and paleoproductivity proxies: an update, Chem. Geol. 232 (1–2) (2006) 12–32, https://doi.org/10.1016/j.chemgeo.2006.02.012.
[44] Y. Song, S. Li, S. Hu, Warm-humid paleoclimate control of salinized lacustrine organic-rich shale deposition in the Oligocene Hetaoyuan Formation of the Biyang Depression, East China, Int. J. Coal Geol. 202 (2019) 69–84, https://doi.org/10.1016/j.coal.2018.11.016.
[45] R.M. Charles, H.N. Kenneth, Bacterial manganese reduction and growth with manganese oxide as the sole electron acceptor, Science 240 (1988) 1319–1321, https://doi.org/10.1126/science.240.4857.1319.
[46] D. Maranguit, T. Guillaume, Y. Kuzyakov, Effects of flooding on phosphorus and iron mobilization in highly weathered soils under different land-use types: short-term effects and mechanisms, Catena 158 (2017) 161–170, https://doi.org/10.1016/j.catena.2017.06.023.
[47] E.C. Donald, Bo Thamdrup, W.H. Jens, The anaerobic degradation of organic matter in Danish coastal sediments: iron reduction, manganese reduction, and sulfate reduction, Geochem. Cosmochim. Acta 57 (16) (1993) 3867–3883, https://doi.org/10.1016/0016-7037(93)90340-3.
[48] J.A. Dearing, R.J. Flower, The magnetic susceptibility of sedimenting material trapped in Lough Neagh, Northern Ireland, and its erosional significance, Limnol. Oceanogr. 27 (5) (1982) 969–975, https://doi.org/10.4319/lo.1982.27.5.0969.
[49] A. Simonneau, E. Doyen, E. Chapron, L. Millet, B. Vannière, C. Di Giovanni, N. Bossard, K. Tachikawa, E. Bard, P. Albéric, M. Desmet, G. Roux, P. Lajeunesse, J. F. Berger, E. Arnaud, Holocene land-use evolution and associated soil erosion in the French Prealps inferred from Lake Paladru sediments and archaeological evidences, J. Archaeol. Sci. 40 (4) (2013) 1636–1645, https://doi.org/10.1016/j.jas.2012.12.002.
[50] Q. Lu, Environment and Indicator Organisms: Water Subvolume, China Environmental Press, 1987, p. 60 (IN CHINESE).
[51] X. Dong, X. Yang, R. Wang, Diatom indicative species of eutrophication of the lakes in the middle and lower reach regions of Yangtze River, China Environ. Sci. 26 (5) (2006) 570–574 (IN CHINESE).
[52] J.M. Reed, Diatom preservation in the recent sediment record of Spanish saline lakes: implications for palaeoclimate study, J. Paleolimnol. 19 (2) (1998) 129–137, https://doi.org/10.1023/A:1007948600780.
[53] R.J. Flower, D.B. Ryves, Diatom preservation: differential preservation of sedimentary diatoms in two saline lakes, Acta Bot. Croat. 68 (2) (2009) 381–399.
[54] T. Hiemstra, Formation, stability, and solubility of metal oxide nanoparticles: surface entropy, enthalpy, and free energy of ferrihydrite, Geochem. Cosmochim. Acta 158 (2015) 179–198, https://doi.org/10.1016/j.gca.2015.02.032.
[55] J. Tao, G. Chen, X. Chen, L. Chen, L. Huang, Y. Liu, H. Shi, K. Hu, J. Wang, W. Kang, Long-term pattern of diatom community responses to water pollution and hydrological regulation in Yangzong Lake, Geogr. Res. 35 (10) (2016) 1899–1911, https://doi.org/10.11821/dlyj201610009 (IN CHINESE).
[56] N. Antia, M. Klut, Fluoride addition effects on euryhaline phytoplankter growth in nutrient-enriched seawater at an estuarine level of salinity, Bot. Mar. 24 (3) (1981) 147–152, https://doi.org/10.1515/botm.1981.24.3.147.
[57] J.T.F. Gillard, A.L. Hernandez, J.A. Contreras, I.M. Francis, L. Cabrales, Potential for biomass production and remediation by cultivation of the marine model diatom phaeodactylum tricornutum in oil field produced wastewater media, Water 13 (19) (2021) 2700, https://doi.org/10.3390/w13192700.
[58] C.M. Joy, K.P. Balakrishnan, Effect of fluoride on axenic cultures of diatoms, Water Air Soil Pollut. 49 (3–4) (1990) 241–249, https://doi.org/10.1007/BF00507067.
[59] K.M. Rühland, A.M. Paterson, J.P. Smol, Lake diatom responses to warming: reviewing the evidence, J. Paleolimnol. 54 (1) (2015) 1–35, https://doi.org/10.1007/s10933-015-9837-3.
[60] R.I. Woolway, C.J. Merchant, J. van den Hoek, C. Azorin-Molina, P. Noges, A. Laas, E.B. Mackay, I.D. Jones, Northern hemisphere atmospheric stilling accelerates lake thermal responses to a warming world, Geophys. Res. Lett. 46 (21) (2019) 11983–11992, https://doi.org/10.1029/2019GL082752.
[61] M.G. Udovic, A. Cvetkoska, P. Žutinić, S. Bosak, I. Stankovic, I. Spoljaric, G. Mrsic, K.K. Borojevic, A. Cukurin, A. Plenkovic-Moraj, Defining centric diatoms of most relevant phytoplankton functional groups in deep karst lakes, Hydrobiologia 788 (1) (2017) 169–191, https://doi.org/10.1007/s10750-016-2996-z.
[62] L. Yao, X. Zhao, G. Zhou, R. Liang, T. Gou, B. Xia, S. Li, C. Liu, Seasonal succession of phytoplankton functional groups and driving factors of cyanobacterial blooms in a subtropical reservoir in South China, Water 12 (4) (2020) 1167, https://doi.org/10.3390/w12041167.